OENO One
VINE AND WINE OPEN ACCESS JOURNAL
By iVES International Viticulture & Enology Society

DOI:10.20870/oeno-one.2022.56.1.4863
OPEN ACCESS

Overcoming the challenge of bunch occlusion by leaves for vineyard yield estimation using image analysis

Gonçalo Victorino[1, 2,*], Ricardo P. Braga[1], José Santos-Victor[2] and Carlos M. Lopes[1]

[1] Linking Landscape, Environment, Agriculture and Food (LEAF), Instituto Superior de Agronomia, Universidade de Lisboa, Lisboa, Portugal
[2] Institute for Systems and Robotics (ISR), Instituto Superior Técnico, Universidade de Lisboa, Lisboa, Portugal

*correspondence:
gvictorino@isa.ulisboa.pt

Associate editor:
Bruno Tisseyre

Received:
30 September 2021

Accepted:
24 January 2022

Published:
4 February 2022

This article is published under the **Creative Commons licence** (CC BY 4.0).

Use of all or part of the content of this article must mention the authors, the year of publication, the title, the name of the journal, the volume, the pages and the DOI in compliance with the information given above.

ABSTRACT

Accurate yield estimation is of utmost importance for the entire grape and wine production chain, yet it remains an extremely challenging process due to high spatial and temporal variability in vineyards. Recent research has focused on using image analysis for vineyard yield estimation, with one of the major obstacles being the high degree of occlusion of bunches by leaves. This work uses canopy features obtained from 2D images (canopy porosity and visible bunch area) as proxies for estimating the proportion of occluded bunches by leaves to enable automatic yield estimation on non-disturbed canopies. Data was collected from three grapevine varieties, and images were captured from 1 m segments at two phenological stages (veraison and full maturation) in non-defoliated and partially defoliated vines. Visible bunches (bunch exposure; BE) varied between 16 and 64 %. This percentage was estimated using a multiple regression model that includes canopy porosity and visible bunch area as predictors, yielding a R^2 between 0.70 and 0.84 on a training set composed of 70 % of all data, showing an explanatory power 10 to 43 % higher than when using the predictors individually. A model based on the combined data set (all varieties and phenological stages) was selected for BE estimation, achieving a R^2 = 0.80 on the validation set. This model did not show validation metrics differences when applied on data collected at veraison or full maturation, suggesting that BE can be accurately estimated at any stage. Bunch exposure was then used to estimate total bunch area (tBA), showing low errors (< 10 %) except for the variety *Arinto*, which presents specific morphological traits such as large leaves and bunches. Finally, yield estimation computed from estimated tBA presented a very low error (0.2 %) on the validation data set with pooled data. However, when performed on every single variety, the simplified approach of area-to-mass conversion was less accurate for the variety *Syrah*. The method demonstrated in this work is an important step towards a fully automated non-invasive yield estimation approach, as it offers a solution to estimate bunches that are not visible to imaging sensors.

KEYWORDS: Grapevine yield prediction, canopy porosity, bunch pixels, proximal sensing, fruit visibility, *Vitis vinifera* L.

INTRODUCTION

Accurate yield estimation is of utmost importance for many commercial crops. In viticulture, such information is helpful to address challenges of logistics at harvest, helping define workforce and machinery required, as well as cellar needs. Furthermore, early yield forecasts can help planning bunch thinning to manage wine stock, grape prices and marketing strategies (Dunn and Martin, 2004). However, vineyard yield estimations can be hard to perform as the amount of fruit can vary highly from season to season as well as spatially across a vineyard (Bramley *et al.,* 2011; Victorino *et al.,* 2017; Jasse *et al.,* 2021). Vineyard yield depends on several factors such as soil and climate conditions, grapevine variety, biotic and abiotic stresses, vineyard management practices (Bramley and Hamilton, 2004; Clingeleffer *et al.,* 2001; Taylor *et al.,* 2018).

One of the most common yield estimation methods involves manually collecting, counting and weighing grape bunch samples at the berry lag phase (BBCH 79, Lorenz *et al.,* 1995). The information is then extrapolated to the whole vineyard or plot, which can cause inaccurate estimates if sampling is not representative enough. Furthermore, it is a destructive and laborious technique (Dunn and Martin, 2004).

There are other methods to estimate vineyard yields, such as pollen-based predictive models (Besselat, 1987; Cunha *et al.,* 2016), static devices that measure wire tension (Blom and Tarara, 2009), or climate data-based models (Fraga and Santos, 2017). However, most of these methods are limited either by the need for high maintenance fixed devices or the scanning of large areas or regions. Recently, machine vision has become a sought-after research topic, as images can be collected massively across a whole vineyard, and data can be georeferenced, helping to understand its spatial variability. Along with quick image collection devices, resulting images can be automatically processed by means of machine learning techniques (Jensen, 1996; Cristianini and Shawe-Taylor, 2000; Lecun *et al.,* 2015), which lead to high throughput systems that can provide real-time data based on image analysis.

In field conditions, image analysis for bunch and berry recognition has been proved to be effective using colour and light thresholding, geometric segmentation and Bayesian approaches (Aquino *et al.,* 2018b; Abdelghafour *et al.,* 2019; Liu *et al.,* 2020), classification algorithms such as Random Forests and Support Vector Machines (Nuske *et al.,* 2014b; Pérez-Zavala *et al.,* 2018) and artificial neural networks (Behroozi-Khazaei and Maleki, 2017; Rudolph *et al.,* 2018; Milella *et al.,* 2019), among others. Three-dimensional imaging has also been explored to compute bunch volume for bunch weight estimation (Font *et al.,* 2015; Ivorra *et al.,* 2015). However, besides being a more complex computer task, Hacking *et al.* (2019) has shown that such technology can yield worse results than 2D imaging, in field conditions, due to the randomness of vine structures and bunch occlusions. Other yield components from earlier phenological stages have also been segmented. Shoots have been automatically identified using unsupervised classification algorithms such as K-means and agglomerative hierarchical clustering (Liu *et al.,* 2017). Flowers and inflorescences have been classified using artificial neural networks (Rudolph *et al.,* 2018) and geometric segmentation inside a Bayesian framework (Abdelghafour *et al.,* 2019). Today, it is generally accepted that these yield components can be accurately identified, and the challenge of analysing vine images for yield component recognition has been overcome (Seng *et al.,* 2018). However, in natural conditions, in general, yield components are not all visible to the scanning sensors, requiring manual intervention (e.g., defoliation) or, alternatively, modelling approaches to estimate non-visible fruits. Regarding the most used yield components for yield estimations with image analysis, there are two main trends that have been explored in previous research: one uses the estimated number of visible berries in an image (Nuske *et al.,* 2014b; Aquino *et al.,* 2018a; Milella *et al.,* 2019; Liu *et al.,* 2020), the other uses bunch projected area or bunch pixels (Liu *et al.,* 2013; Lopes *et al.,* 2017; Hacking *et al.,* 2020; Victorino *et al.,* 2020).

Bunch occlusion by leaves is common in grapevines, especially in dense canopies. It prevents bunches from being overly exposed to sun radiation which, if in excess, can cause losses in berry quality and sunburn damage (Gambetta *et al.,* 2021). From an image analysis perspective, however, leaf coverage is a limitation as it causes a large percentage of bunches to be occluded from the imaging devices. As it has been pointed out by Nuske *et al.* (2014a), berries can be occluded by leaves, wooden material and neighbouring berries. The same authors name these occlusions as self-occlusions (berry by berry), cluster-occlusions (berry by bunches) and vine-occlusions (berry by leaves and shoots). In the present work, the authors opted to address yield estimation by exploring the vine bunch projected area; however, occlusions can occur regardless of the considered yield component. Vine-occlusions appear to be the main challenge (Victorino *et al.,* 2019; Íñiguez *et al.,* 2021), particularly leaf-occlusions, especially in dense canopies that present numerous leaf layers (Smart and Robinson, 1991).

To overcome the challenge of fruit bunch occlusion, previous works have performed yield estimation using image analysis on vines that were defoliated prior to image collection (e.g. Dunn and Martin, 2004; Pérez-Zavala *et al.,* 2018; Milella *et al.,* 2019), with the exception of works developed at very early phenological stages (Liu *et al.,* 2017). Grapevine basal leaf removal is a canopy management practice mainly used in viticulture regions where a higher bunch sun exposure is desired to reduce canopy density and improve fruiting area ventilation and luminous microclimate to reduce fungi pressure and improve polyphenolic composition in red grapes (Lopes *et al.,* 2020). However, in warm climate viticulture, such practices are not as common, considering the increasing instability caused by climate change. The higher sun exposure caused by defoliation can lead to increased berry temperature, negatively impacting berry composition and, ultimately, to berry sunburn, which can lead to great yield

losses (Martínez-Lüscher *et al.,* 2020). Furthermore, leaf removal is an expensive and time-consuming management practice, and yield estimation methods cannot be dependent on it. Nuske *et al.* (2011a) estimated an occlusion ratio either by sampling a small number of vines at the time of image collection or using occlusion ratios estimated from previous harvests. However, this methodology is not fully automatic as it still depends on manual sampling. Riggio *et al.* (2018) used another approach consisting of an imaging system to collect images from under the canopy, in an upwards perspective. This is a promising methodology to overcome leaf occlusion, yet it was developed on a very particular training system (Geneva double curtain) where the location of the bunches in relation to the vegetation is much different (downward shoot positioning) than in the most common training systems such as the vertical shoot positioning. Recently, Kierdorf *et al.* (2021) developed an algorithm to estimate hidden berries based on artificially generated images of occluded fruits, reducing the need for natural images and the labour associated with their collection and labelling. The algorithm showed promising yet inconclusive results when applied to non-synthetic data (real vine images). Another technology was tested by Parr *et al.* (2021), where ultrasonic phased arrays were used to overcome the problem of occluded bunches, showing results that appear promising in controlled conditions. However, despite all these research efforts, the challenge of bunch occlusion in vineyard conditions remains unsolved.

Grapevine canopy porosity (POR) is defined as the proportion of gaps in the canopy where no plant material is present (Smart, 1987; Diago *et al.,* 2019). This POR, when determined at the fruit zone, shows a positive correlation with fruit exposure (Smart, 1988), indicating that the more gaps the canopy has, the more fruit will be potentially visible. Canopy porosity can be influenced by several factors like shoot density, shoot leaf area water availability, biotic and other abiotic stresses, among others and has been shown to influence fruit exposure to sunlight and, hence, berry health and composition (Smart, 1987; Austin *et al.,* 2011). In warm climates, a lower POR can decrease the risk of berry sunburn, as more leaves cover bunches from direct sunlight (Krasnow *et al.,* 2010). Canopy porosity is commonly manually assessed using the Point Quadrat method (Smart and Robinson, 1991), but recently it has been proven that it can be estimated with accuracy in a more automatic and objective method via image analysis (De Bei *et al.,* 2016; Diago *et al.,* 2019).

Based on the above-stated assumption that a relationship between canopy porosity and exposed bunches exists, the present work aims at testing the use of canopy traits (porosity and visible bunch area) as proxies for estimating the proportion of occluded bunches by leaves and, hence, overcoming the main difficulty faced by proximal remote sensing devices used for estimating vineyard yield.

MATERIALS AND METHODS

1. Plant material and growth conditions

The experiment was carried out in two fully grown experimental vineyards in the Lisbon winegrowing region, Portugal (Figure 1). Data were collected at Instituto Superior de Agronomia (ISA) vineyard, located at Tapada da Ajuda (38°42'24.61" N 9°11'05.53" W).



FIGURE 1. Location of studied vineyard plots (1 and 2) in Lisbon, Portugal at 38°42'24.61" N 9°11'05.53" W. Image acquired from Google Earth®.

The climate is of Mediterranean type with an Atlantic influence. This vineyard includes two different plots with spur pruned vines trained on a vertical shoot positioning trellis system with two pairs of movable wires. The first plot includes two drip-irrigated white varieties ('Encruzado' and 'Arinto') grafted onto 1103 Paulsen rootstock, planted side by side in 2006 and spaced 1.0 m within and 2.5 m between north–south oriented rows. Water was supplied with a drip irrigation system, and irrigation was managed using a soil moisture sensor. Readily available water was maintained until veraison, at which point stress was applied by replacing only 50 % of crop evapotranspiration. The second plot is rainfed and consists of the 'Syrah' variety (grafted onto 140 Ruggery rootstock) planted in 1999 and spaced 1.2 m within and 2.5 m between north–south oriented rows. In both plots, the soil is a clay loam with approximately 1.6 % organic matter and a pH of 7.8 (Teixeira *et al.,* 2018). Data were collected from both plots in 2018 (except 'Arinto') and 2019. On the two seasons, both plots were subject to similar standard cultural practices during the growing cycle, including shoot trimming at 1.2 m above the cordon, water shoot removal, shoot positioning and fertilization.

Data were collected during the 2018 ('Encruzado' and 'Syrah' varieties) and 2019 ('Encruzado', 'Syrah' and 'Arinto' varieties) seasons. A total of 140 one-meter canopy segments (corresponding to the row space, 1 vine) were imaged and assessed in both seasons (70 at veraison and 70 at harvest), distributed along the vineyard to encompass as much spatial variability as possible.

The 2018 season was characterised by a wet spring (~300 mm of precipitation from March to June) and a warm and dry summer (~15 mm of precipitation and average mean temperature of 22.1° C, from June to September), whereas the 2019 season presented a drier spring (~119 mm of precipitation from March to June) and a dry and warm summer (~17 mm of precipitation and average mean temperature of 20.6 °C, from June to September).

2. Image acquisition

Grapevine images were collected in a lateral perspective using a commercial camera (Nikon D5200) equipped with a Sigma 50 mm F2.8 macro (Sigma corp., Kanagawa, Japan), set to auto-mode. RGB images were saved at a resolution of 24 Mpx (6000 × 4000 pixels), 8 bits per channel and with uncontrolled illumination. The camera was mounted on a tripod approximately 2 m away from the row axis and 1 m above the ground (Figure 2). A blue background was placed behind the canopy for each imaged canopy segment.

Images were collected in 2018 and 2019 at two phenological stages: veraison (BBCH 81) and harvest (BBCH 89). These phenological stages corresponded approximately to 1 month and 1 week prior to harvest, respectively. For more details, see Victorino *et al.* (2020).

Images were firstly collected on undisturbed canopies, followed by partial defoliation at the fruit zone to simulate a broader range of porosity situations. Afterwards, vines were fully defoliated to uncover all bunches occluded by leaves (Figure 2D–F).

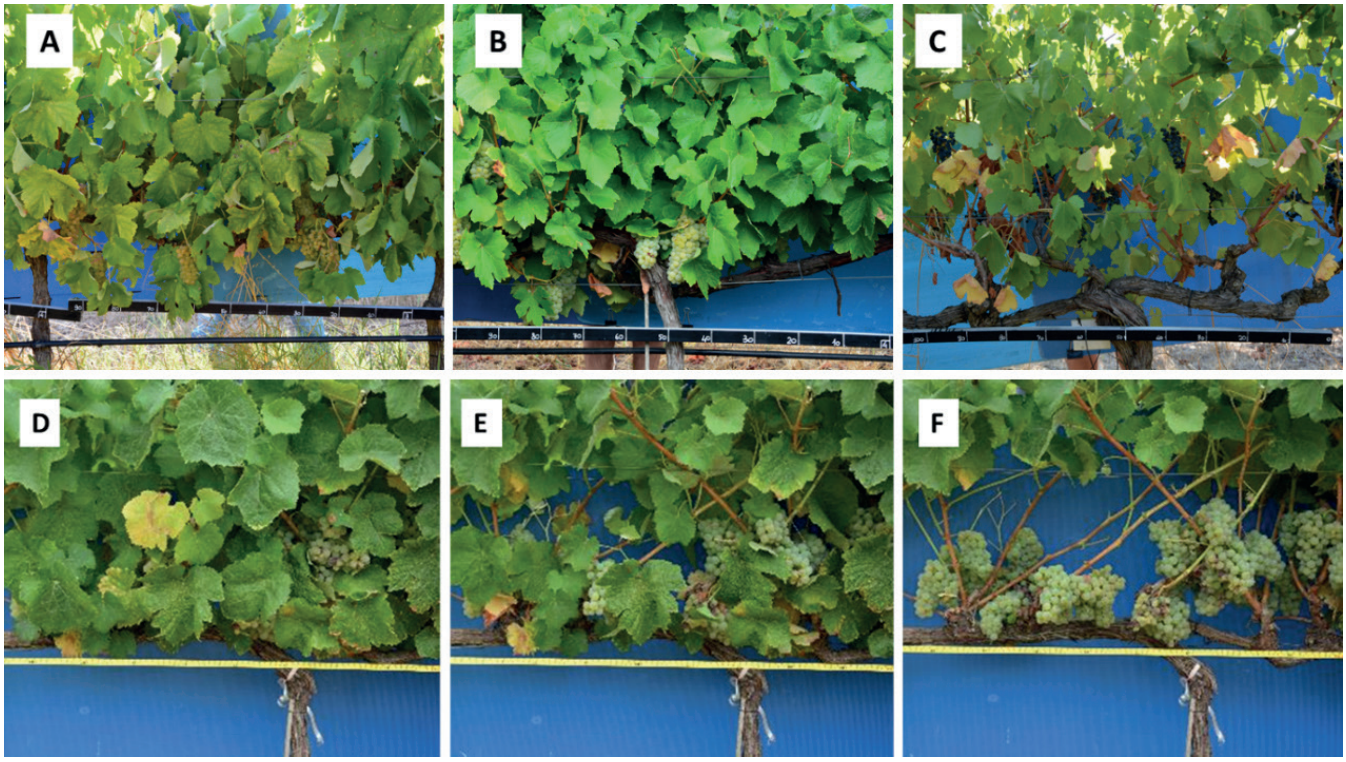


FIGURE 2. Images collected in a lateral perspective with a blue background near harvest.

(A) variety *Arinto*; (B) variety *Encruzado*; (C) variety *Syrah*. Images collected at different defoliation steps on a dense canopy segment of the variety *Encruzado* near harvest (2018). (D) non-defoliated; (E) partially defoliated; (F) fully defoliated.

A total of 270 images were collected in analysed in this work. After image collection, all bunches were picked and weighed per canopy segment, and fruit mass was determined at each analysed phenological stage. To avoid direct light incidence and consequent poor-quality imaging, images were collected after midday, taking advantage of the north–south row orientation and the shade provided by the background positioned on the opposite side of the canopy combined with the fully developed canopy.

3. Image processing

A region of interest of 50 cm above the cordon was defined for each image for detailed analysis (Figure 3A). On each image, pixels of leaves, bunches, canopy gaps and wooden organs could be found. Bunch segmentation was performed manually for each individual image to obtain the true bunch projected area in the image for each canopy segment (Figure 3B and C). Segmentation was performed using the software ImageJ® (v1.52e, National Institutes of Health, EUA). Canopy gap pixels were classified using a static colour threshold after converting the original image from RGB to HSV (Hue–Saturation–Value) colour space for improved invariance to illumination conditions. The algorithm was developed using OpenCV in PyCharm®, an open-source Python-focused IDE, for automation purposes.

4. Data analysis

Data were divided into two sets: the training set, which included 70 % of all non-defoliated and partially defoliated vine images and the validation set, which included the remaining 30 %. In both the training and validation sets, data were organized according to variety and phenological stage to further explore the analysis. Several variables were addressed as follows: visible bunch area in cm^2/m (vBA) and in proportion to the whole image (vBA_p), described as the projected area of non-occluded bunches (Figure 3C in yellow); total bunch area (tBA), in cm^2/m, defined as the projected area of non-occluded bunches, assessed after full defoliation; bunch exposure (BE), in percentage, described as the ratio between vBA and tBA; canopy porosity (POR),

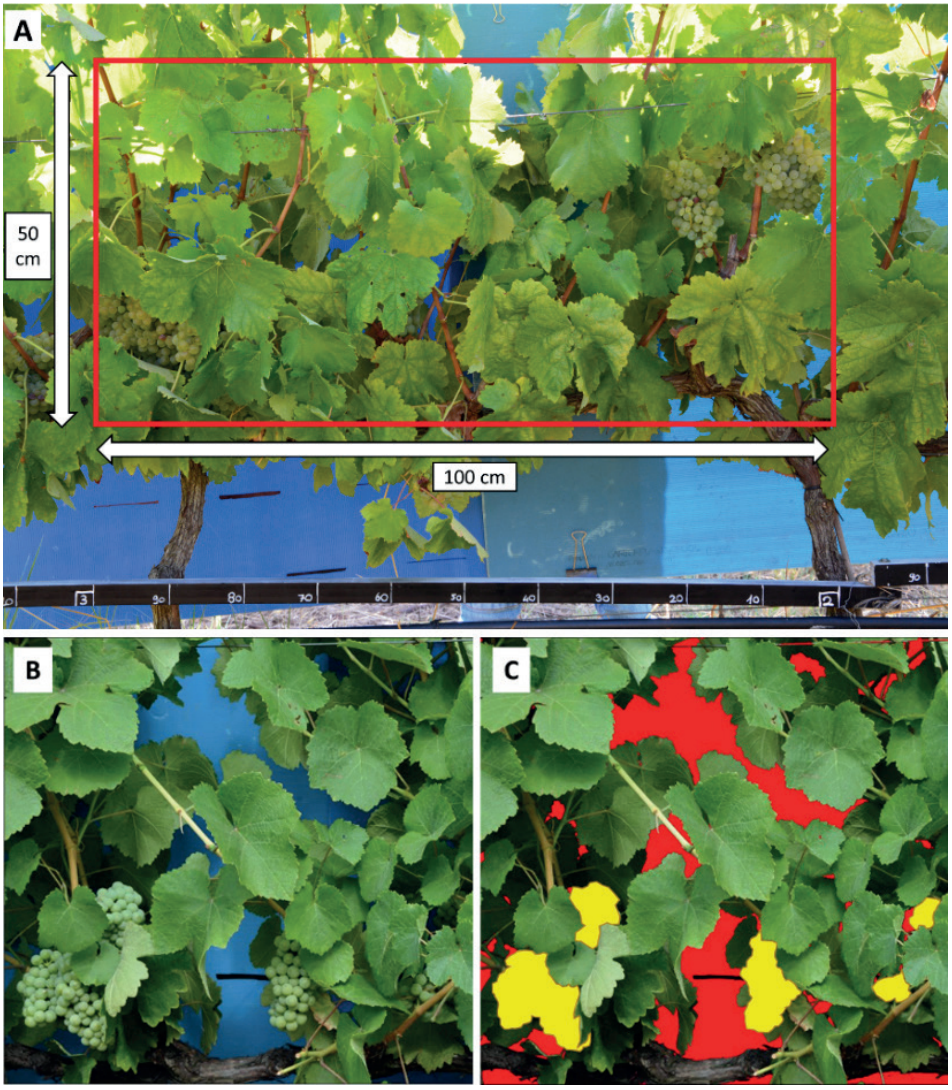


FIGURE 3. (A) Example of an analysed image obtained from the variety *Arinto* at harvest and respective region-of-interest for image analysis. Canopy porosity and bunch segmentation computed on the same canopy segment of *Encruzado* variety at veraison: (B) original image; (C) canopy gaps pixels (in red) and bunch pixels (in yellow).

in percentage, described as the percentage of canopy gaps at the fruiting zone (Eq. 1; Figure 3C in red); fruit mass (FM), in kg/m, described as the actual bunch mass assessed for the corresponding image.

Descriptive statistics were computed for both data sets together (Table 1). Total bunch area (tBA) corresponds to the visible bunch area (vBA) of the fully defoliated vine segment. Canopy porosity and visible bunch area were selected as the main variables to estimate bunch exposure (BE). Canopy porosity (POR) was estimated according to Equation 1, in which the number of total pixels corresponds to the entire image (including canopy gaps, grapes, leaves, shoots and old wood). As this work focuses on occlusions caused by leaves, other types of occlusions, such as bunch occlusions by other bunches or shoots, were not considered.

$$\text{POR (\%)} = \frac{\text{(Number of gap pixels)}}{\text{(Number of total pixels)}} \times 100 \qquad (1)$$

On the training set, for each variety and phenological stage, a linear model was fitted between POR, vBA_p (predictor variables) and BE (response variable), only on data from images of non-defoliated and partially defoliated vines. Then, a multiple linear regression between the same predictors and response variables was fitted. Models were computed, and variables were transformed according to maximum likelihood analysis performed in SAS®. For validation, to evaluate the final model goodness of fit to the observed data, the following deviance measures were used: bias (Eq. 2), mean absolute percentage error (MA%E, Eq. 3), root mean square error (RMSE, Eq. 4) and modelling efficiency (EF, Eq. 5). A regression analysis of actual vs. estimated data and the F-test for slope = 1 and for intercept = 0 were performed for model evaluation.

$$\text{Bias} = \sum(y_i - \hat{y}_i)/n \qquad (2)$$

$$\text{MA\%E} = 100 \times [\sum(|y_i - \hat{y}_i|/|y_i|)]/n \qquad (3)$$

$$\text{RMSE} = \sqrt{(\sum(y_i - \hat{y}_i)^2/n} \qquad (4)$$

$$\text{EF} = 1 - \frac{\sum(y_i - \hat{y}_i)^2}{\sum(y_i - \bar{y})^2} \qquad (5)$$

where y_i represents observed values, $\hat{y}_i$ estimated values, $\bar{y}$ average observed value and n the number of pairs.

Estimated tBA was calculated using Equation 6. Fruit mass was estimated based on the relationship between observed tBA and observed fruit mass (from the training set) at vine level, an approach similar to the one mentioned in Lopes *et al.* (2016) and Victorino *et al.* (2020).

TABLE 1. Average ± standard error of the variables assessed on different varieties (Var) at veraison (Ver) and harvest (Harv) for different levels of canopy defoliation at fruiting area, for the training and validation set combined.

Var	Phen. stage	DEF	n	vBA (cm²/m)	vBA_p (%)	POR (%)	BE (%)	FM_{act} (kg/m)
		None	20	128.8 ± 21.2	2.6 ± 0.4	6.9 ± 1.1	15.8 ± 1.8	
Arinto	Ver	Partial	20	324.8 ± 43.2	6.5 ± 0.9	17.5 ± 2.4	41.8 ± 3.5	2.1 ± 0.2
		Total	20	780.5 ± 73.3	15.6 ± 1.5	70.0 ± 1.3	100 ± 0.0*	
		None	25	134.1 ± 15.3	4 ± 0.5	8.1 ± 1.3	19.8 ± 1.7	
Enc.	Ver	Partial	24	338.4 ± 27.4	8.7 ± 0.9	16.6 ± 1.6	53.4 ± 3.0	1.9 ± 0.1
		Total	25	656.0 ± 39.4	17 ± 1.2	58.9 ± 1.6	100 ± 0.0*	
		None	25	116.2 ± 11.7	2.7 ± 0.3	9.0 ± 0.9	20.9 ± 1.7	
Syrah	Ver	Partial	25	249.6 ± 22.3	6.8 ± 0.5	18.9 ± 1.1	45.0 ± 2.9	0.8 ± 0.1
		Total	25	546.5 ± 36.8	13.1 ± 0.8	68.4 ± 1.2	100 ± 0.0*	
		None	20	200.6 ± 25.6	3.8 ± 0.5	7.0 ± 0.9	22.6 ± 1.9	
Arinto	Harv	Partial	20	432.6 ± 47.2	7.6 ± 0.6	17.7 ± 2.0	50.3 ± 3.6	3.7 ± 0.3
		Total	20	851.1 ± 59.8	14.4 ± 1	68.3 ± 1.4	100 ± 0.0*	
		None	26	189.6 ± 24.3	2.3 ± 0.2	9.9 ± 1.2	25.9 ± 2.6	
Enc.	Harv	Partial	26	379.1 ± 31.6	5 ± 0.4	20.0 ± 1.4	53.8 ± 3.1	3.0 ± 0.3
		Total	26	719.9 ± 50.2	10.9 ± 0.7	61.0 ± 1.8	100 ± 0.0*	
		None	26	228.6 ± 26.7	3.3 ± 0.5	14.2 ± 1.7	43.2 ± 4.4	
Syrah	Harv	Partial	26	336.7 ± 37.3	4.9 ± 0.7	25.2 ± 2.6	63.9 ± 6.4	1.3 ± 0.1
		Total	26	566.4 ± 39.0	11.3 ± 0.8	68.0 ± 1.2	100 ± 0.0*	

n: number of observations. DEF: defoliation intensity. Fruit mass (FM_{act}) is shown per data set as it is the same for each defoliation step. vBA = visible bunch area; vBAp = proportion of visible bunch area in the image; POR = canopy porosity; BE = Bunch exposure.
*with total defoliation, there is no occlusion caused by vegetation.

Both variables (estimated tBA and estimated fruit mass) were evaluated by analysing the relative mean error (Eq. 7).

$$\text{Estimated tBA (cm}^2\text{/vine)} = 100 \times \frac{vBA\ (\text{cm}^2\text{/vine})}{\text{estimated BE (\%)}} \quad (6)$$

$$\text{Relative mean error (\%)} = 100 \times \frac{1}{n} \times \sum(y_i - \hat{y}_i / y_i) \quad (7)$$

RESULTS

1. Estimation of occluded bunch area

In fully defoliated vines, tBA presented a Pearson correlation coefficient of 0.78 with fruit mass. In the proposed methodology, the authors estimate fruit mass by first estimating tBA through BE (Eq. 6). It is important to reference again that the BE does not consider bunch occlusion by other bunches, but only bunch occlusion by leaves.

Figure 4 shows the relationship between POR and vBA_p with BE on images taken on non-defoliated and partially defoliated vines of the training data set. Visual observation shows that there is a linear trend between POR and BE (Figure 4A). A similar trend is also observed in Figure 4B between vBA_p and BE but with variability that increases with the increase in the magnitude of BE. Regression models were computed using POR and vBA_p as predictors of BE (Table 2). For both relationships, a maximum likelihood analysis suggested that a root transformation of the response variable (BE) would be more appropriate than the original scale in some data sets. The resulting models, after converting the rooted response variable back to the original scale, corroborate the visual appraisal of the scatter plot. Indeed, both regression models present a high and significant R^2 ($p < 0.001$) for every single variety and the combined data. For the POR predictor, the *Syrah* dataset presented the highest R^2 of all varieties, followed by *Encruzado* and *Arinto*. When comparing both phenological stages, a higher R^2 was observed at harvest. Regarding the vBA_p predictor, the *Syrah* dataset also presented the highest R^2 between all varieties, followed by

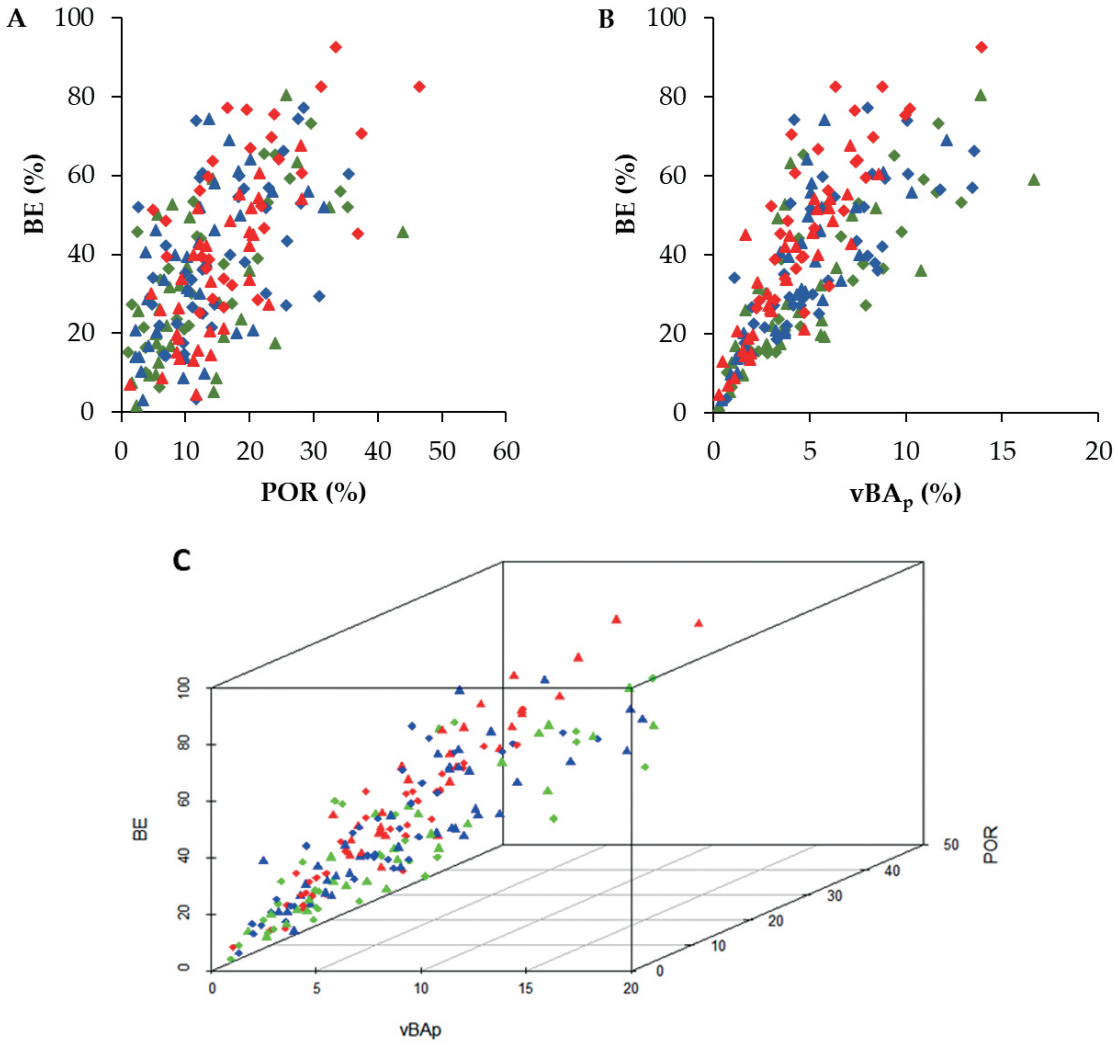


FIGURE 4. Scatterplots between bunch exposure (BE) over (A) canopy porosity (POR), (B) visible bunch area (vBAp) in 2D and 3D (C), for the three studied varieties at two phenological stages (veraison and harvest).

All plots were computed using data from non-defoliated and partially defoliated vines of the training set. Marker codes: Triangles = Veraison (n = 97); Diamonds = Harvest (n = 107); Green = *Arinto* var. (n = 57); Blue = *Encruzado* var. (n = 73); Red = *Syrah* var. (n = 74).

TABLE 2. Fitted models from the fitted regressions between bunch exposure (BE) over canopy porosity (POR) and percent visible bunch area (vBAp).

ID	Predictors	Variety	Stage	n	Fitted model	R^2
1	POR	*Encruzado*	Combined	73	BE = 19.97 + 1.278*POR	0.30
2		*Syrah*	Combined	74	BE = 15.23 + 1.6224*POR	0.45
3		*Arinto*	Combined	57	$BE = (4.051 + 0.108*POR)^2$	0.37
4		Combined	Veraison	97	$BE = (3.9 + 0.121*POR)^2$	0.30
5		Combined	Harvest	107	BE = 15.23 + 1.6224*POR	0.41
6		Combined	Combined	204	$BE = (8.627 + 0.424*POR)^{1.333}$	0.38
7	vBA_p	*Encruzado*	Combined	73	$BE = (3.791 + 0.411* vBA_p)^2$	0.59
8		*Syrah*	Combined	74	$BE = 11.56 + 6.74* vBA_p$	0.74
9		*Arinto*	Combined	57	$BE = (3.584 + 0.36* vBA_p)^2$	0.58
10		Combined	Veraison	97	$BE = (3.617 + 0.36* vBA_p)^2$	0.57
11		Combined	Harvest	107	$BE = (4.24 + 0.364* vBA_p)^2$	0.51
12		Combined	Combined	204	$BE = (3.864 + 0.409* vBA_p)^2$	0.56
13	POR & vBA_p	*Encruzado*	Combined	73	$BE = (1.245 + 1.71*\sqrt{vBA_p} + 0.28*\sqrt{POR})^2$	0.70
14		*Syrah*	Combined	74	$BE = 2.368 + 5.50* vBA_p + 0.88*POR$	0.84
15		*Arinto*	Combined	57	$BE = (1.009 + 1.45*\sqrt{vBA_p} + 0.41*\sqrt{POR})^2$	0.73
16		Combined	Veraison	97	$BE = (0.899 + 1.74*\sqrt{vBA_p} + 0.36*\sqrt{POR})^2$	0.73
17		Combined	Harvest	107	$BE = (0.96 + 1.45*\sqrt{vBA_p} + 0.53*\sqrt{POR})^2$	0.70
18		Combined	Combined	204	$BE = (0.853 + 1.60*\sqrt{vBA_p} + 0.46*\sqrt{POR})^2$	0.73

All R^2 are statistically significant at $p < 0.001$.

Encruzado and *Arinto*, which presented very similar values among them. As opposed to the POR relationship, a higher R^2 was observed at the veraison phenological stage than near harvest. In general, the highest R^2 was observed in the models with vBA_p as a predictor, with models based on the combined data set having a R^2 of similar magnitude as the individual cases.

Figure 4C presents a scatterplot where the two predictors (POR and vBA_p) are plotted with BE. Visual observation shows that the combined variables tend to explain BE better than each one, individually. Most *Syrah* dataset observations are plotted in the upper left side of the plot, indicating a possible variety effect. No phenological stage effect is apparent. As in the previous chapter, for all data sets (except *Syrah*), a maximum likelihood analysis suggested that a square root transformation of the response variable (BE) would be more appropriate than the original scale. The resulting models, after converting the square rooted response variable back to the original scale, are presented in Table 2, along with their respective R^2. All models present a significantly high R^2, corroborating the visual appraisal, with the highest value being observed for the *Syrah* dataset, followed by *Arinto* and *Encruzado*. Models from the two phenological stages presented very similar results. The model based on the pooled data from all data sets (Table 2, nº 18) presents a R^2 of similar magnitude to all other cases. Furthermore, model 18 was computed with a larger number of images, thus possibly making it more robust to different stages or varieties. Even though there are slight differences between the variety *Syrah* and the remaining ones, the authors still opted for this model as it provides a generalized option that goes in accordance with the objectives of this work. This generalisation hypothesis is tested and discussed further ahead.

2. Model validation

To test the potential of the model based on pooled data (model 18, Table 2), a validation was performed on a data set which, such as the training set, was separated by variety, stage and with all cases combined (Figure 5 and Table 3). Visual observation shows an overall good agreement between observed and actual values for all varieties and stages, especially at low values of BE, but also some variability in cases of medium BE magnitude (between 40 % and 70 % of BE). The statistical measures of validation corroborate the good fit (Table 3). When comparing the models fitted between observed and estimated values among varieties, the selected model showed a slightly lower MAE for the *Syrah* dataset compared to the other varieties while having approximately the same RMSE for all cases. The *Encruzado* model presented the lowest absolute Bias among varieties, and the highest EF of all cases, while the

Arinto model showed the highest absolute Bias, followed by *Syrah*, and an EF which was higher than that of *Syrah* but lower than that of *Encruzado*. Regarding the models fitted for each phenological stage, all statistic measures of validation presented similar magnitudes. Overall, the selected model showed good performance on all data sets, presenting an average overestimation only on the *Arinto* data set and an average underestimation on the *Syrah* data set of similar magnitude. When the complete validation data set was considered (combined), statistical indicators were not different from most single data sets, highlighting the fact that it presented a Bias very close to 0.

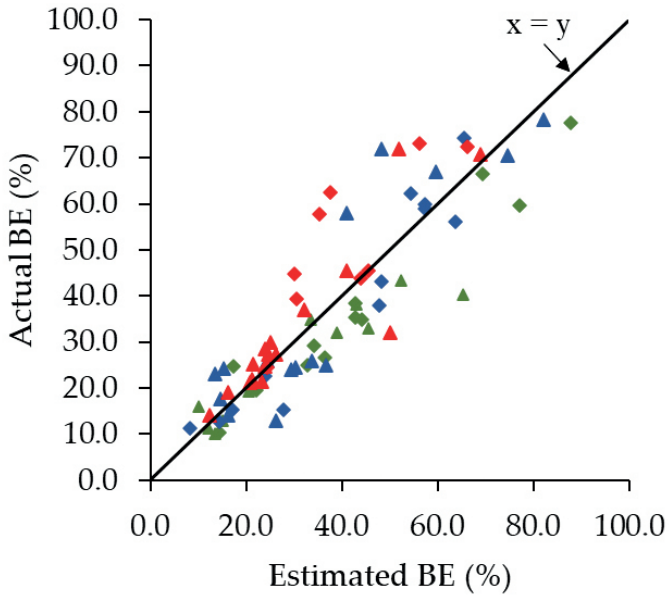


FIGURE 5. Relationship between actual and estimated bunch exposure (BE) obtained using the elected model (Table 2, model 18) on the validation set.

Black line represents the 1:1 line. Marker codes: Triangles = Veraison (n = 42); Diamonds = Harvest (n = 33); Green = *Arinto* var. (n = 23); Blue = *Encruzado* var. (n = 27); Red = *Syrah* var. (n = 27).

TABLE 3. Statistical measures of validation of the model are presented in Table 2 (model 18) for bunch exposure (BE) estimation. RMSE = root mean square error, MAE = mean absolute error, EF = modelling efficiency.

Variety	Phenol. Stage	n	Linear regression		R^2	RMSE (%)	MAE (%)	Bias (%)	EF
			Slope[1]	Intercept[2]					
Encruzado	Combined	27	1.09 $^{n.s.}$	2.26 $^{n.s.}$	0.83***	12.60	11.59	0.61	0.84
Syrah	Combined	25	1.02 $^{n.s.}$	–0.62 $^{n.s.}$	0.81***	12.21	7.95	–6.43	0.73
Arinto	Combined	23	0.78***	2.64 $^{n.s.}$	0.91***	12.69	11.14	8.04	0.78
Combined	Veraison	42	0.91$^{n.s.}$	2.89 $^{n.s.}$	0.79***	13.12	10.46	0.30	0.77
Combined	Harvest	33	0.93 $^{n.s.}$	3.17 $^{n.s.}$	0.80***	11.79	9.96	0.28	0.80
Combined	Combined	75	0.92$^{n.s.}$	2.79$^{n.s.}$	0.80***	12.49	10.24	0.29	0.80

[1]F-test for slope = 1; [2]F-test for intercept = 0; n.s.: not significant; *** $p < 0.001$.

3. Fruit mass estimation

To perform final fruit mass estimations based on the estimated BE obtained from the above-described model, two other steps were required. First, BE was converted to estimated tBA using Equation 6. Table 4 shows the estimated summed values of tBA (sum of all considered 1 m vine segments) and respective percentage errors for the validation set, considering all dataset cases, in this case, separated by phenological stage, inside each variety. When comparing the errors, the *Syrah* harvest dataset presented the largest absolute error, followed by *Arinto* harvest and then *Arinto* veraison data sets. The variety *Syrah* was the only one with overall overestimations of tBA. The *Encruzado* veraison data set showed the lowest absolute tBA estimation error, followed by *Syrah* veraison and then *Encruzado* harvest. Regarding the comparison among the two phenological stages (with combined varieties), both cases presented low errors, with the veraison data set having a slightly lower absolute error than the harvest data set. Considering the combined data set for both variety and phenological stage, the summed estimated tBA presented a low error of estimation, below 5 %.

TABLE 4. Summed values of estimated total bunch area (tBA_{est}) and estimated fruit mass (FM_{est}) on the validation set, and respective area-to-mass conversion equations and relative mean error (Eq. 7).

Variety	Phenol. Stage	n	Area-to-mass equation	tBA		Fruit mass	
				tBA_{est} (cm^2)	Error (%)	FM_{est} (kg)	Error (%)
Encruzado	Veraison	15	$Y_{est} = 2.9*tBA_{est}$	10,064.1	–0.9	29.1	–0.4
Encruzado	Harvest	12	$Y_{est} = 4.2*tBA_{est}$	8228.1	–7.3	34.9	–12.0
Syrah	Veraison	16	$Y_{est} = 1.6*tBA_{est}$	9427.5	4.7	14.7	14.1
Syrah	Harvest	9	$Y_{est} = 2.3*tBA_{est}$	5490.1	18.7	12.8	36.1
Arinto	Veraison	11	$Y_{est} = 2.7*tBA_{est}$	7573.4	–16.1	20.5	–12.9
Arinto	Harvest	12	$Y_{est} = 4.3*tBA_{est}$	9460.5	–17.7	40.8	–17.5
Combined	Veraison	42	$Y_{est} = 2.5*tBA_{est}$	27,065.0	–3.2	65.0	3.6
Combined	Harvest	33	$Y_{est} = 3.9*tBA_{est}$	23,178.7	–5.4	95.2	–5.3
Combined	*Combined*	75	$Y_{est} = 3.2*tBA_{est}$	50,243.7	–4.2	160.2	0.2

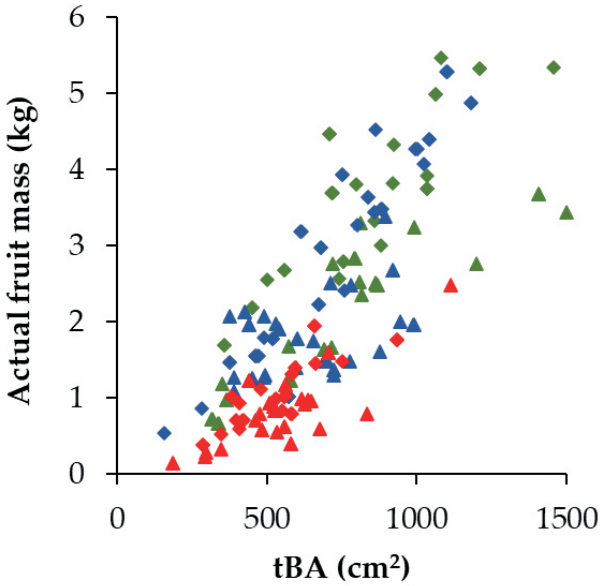


FIGURE 6. Scatterplot between actual vine fruit mass over actual total bunch area (tBA) for the three studied varieties at two phenological stages.

Plot computed using data from fully defoliated vines of the training set. Marker codes: Triangles = Veraison (n = 50); Diamonds = Harvest (n = 47); Green = *Arinto* var. (n = 29); Blue = *Encruzado* var. (n = 31); Red = *Syrah* var. (n = 37).

After estimating tBA, the next step towards fruit mass estimation lies in the conversion of tBA into weight. Figure 6 shows the relationship between actual tBA and fruit mass at the analysed phenological stage. Visual observation shows that there is a linear trend between the two variables; however, the disposition of the *Syrah* observations (in red) hints at a possible variety dependency, while there also seems to be a trend that separates observations at veraison from harvest. Because of this, using the training set, individual regression models between actual tBA (predictor variable) and actual fruit mass (response variable) were fitted for each data set and are presented in Table 4 (area-to-mass equation). For simplification reasons, the regression intercept was set to zero.

The estimated values for the summed fruit mass on the validation set and respective relative mean error, separated by variety, stage and all data combined, are also shown on Table 4. The *Encruzado* veraison data set presented, by far, the lowest absolute error, followed by *Encruzado* harvest and then *Arinto* veraison. The highest absolute errors were shown by the *Syrah* harvest data set, followed by *Arinto* harvest. *Syrah* is also the only variable data set with an overestimation of fruit mass. Regarding the comparison between the two phenological stages for combined varieties, the data set at veraison presented a very slight overestimation of fruit mass, while at harvest, there was a low underestimation. The combined data set presented an error that was very close to zero.

DISCUSSION

In the present work, canopy traits such as porosity and visible bunch area are used as proxies for estimating the proportion of occluded bunches in vine images. The linear trend presented by the point cloud between POR and BE (Figure 4A) hints that bunch occlusion can be indirectly estimated from image-based canopy traits. This relationship was first demonstrated by the works of Richard Smart based on the use of the Point Quadrat method to evaluate canopy porosity (Smart, 1987). In recent work, we have applied this idea with success for the varieties *Encruzado* and *Syrah* (Victorino *et al.,* 2019), and the topic has been generally discussed in Victorino *et al.* (2020). However, even though the models presented in Table 2 (ID 1 to 6) present medium R^2, the percentage of bunch exposure variability explained by POR was still too low to enable an accurate estimation of BE, as it was preliminarily explored in (Victorino *et al.,* 2019). Furthermore, POR itself, when calculated using image analysis (Diago *et al.,* 2019) or even LiDAR technology (Pfeiffer *et al.,* 2018), has a chance to be misestimated if canopy gaps are occupied by bunches. This can be increasingly problematic in cases of low canopy porosity and high yield, where BE would likely be underestimated. So far, research on this subject sidestepped the challenge of bunch occlusion by leaves by fully defoliating the fruit zone and focusing exclusively on the automatic bunch segmentation issue (Dunn and Martin, 2004; Nuske *et al.,* 2011b; Riggio *et al.,* 2018; Pérez-Zavala *et al.,* 2018; Milella *et al.,* 2019). If bunch pixels in the image are also considered, some of these limitations can potentially be overcome.

Aquino *et al.* (2018b) mention that the randomness of bunch exposure causes vBA to be considered an unreliable predictor of yield. In (Íñiguez *et al.,* 2021), a similar trend was observed for the variety Tempranillo, in Spain, with vBA in non-defoliated vines having a low correlation with yield. However, this may only be true if the variable is considered individually. By itself, the relationship between vBA_p and BE showed high R^2 values (Table 2, ID 7 to 12), yet there is an increase in variability at higher magnitudes (Figure 4B). This variability increase was slightly less visible with the variety *Syrah*. However, we suspect that the cause for a better agreement in its regression model with BE is not caused by the variety difference but the fact that in our work, the variety *Syrah* is rainfed and presents less vegetative vigour. Indeed, it is plausible to suspect that the challenge of estimating occluded bunches would be easier to overcome in less vigorous conditions, as a smaller percentage of bunches are occluded (Keller *et al.,* 2016)

The *Syrah* model was the only case where a maximum likelihood analysis did not suggest a square root transformation to the response variable in a multi-variable scenario (Table 2). As mentioned above, we suspect this behaviour might be due to water stress and higher bunch exposure and not a varietal difference. Apart from this case, no other individual variety or stage fitted model presented a higher R^2 than when all data were combined, suggesting the viability of model 18 (Table 2) to be used across different varieties and stages.

When validating model 18, the variety *Arinto* stood out as being the data set on which the model presented the highest overestimation of BE. In fact, almost all *Arinto* observations are below the 1:1 line, regardless of the phenological stage (Figure 5). Such a trend can possibly be explained by the impact of this variety's large leaves and large bunches (OIV, 2009) on bunch occlusion. Indeed, larger leaf surfaces have a higher chance to cover bunches and decrease POR on non-disturbed canopies (e.g., Table 1). Furthermore, in a 2D image, large bunches are more prone to be occluded by other bunches (especially when there is a high density of bunches in the fruiting zone) and to have more berries occluded by other berries inside the same bunch (berry by berry occlusion) as shown in Table 1 (lower observed BE, before defoliation at all stages). However, even with these differences, the variety *Arinto* still showed a vBA_p higher than other varieties at harvest before defoliation. The lowest bias and highest EF presented by the variety *Encruzado* data set seems to corroborate this hypothesis. Compared to the other varieties, *Encruzado* presents average sized bunches and leaves (OIV, 2009) and showed medium values of POR and vBA_p (Table 1). This suggests that model 18 can be particularly effective in varieties with morphologic traits similar to the ones presented by *Encruzado* in our study. Furthermore, the data set of the variety *Syrah* was the only one on which the model underestimated BE, which is mostly due to data collected at harvest (Table 3 and Figure 5). This suggests that this variety's image features are different from the other cases, especially at harvest, which can have two potential reasons. The first reason is the higher observed POR, indicating a sparser canopy (Table 1). In fact, at harvest, the variety *Syrah* shows 5 to 7 % higher POR than the other two varieties, either before or after partial defoliation. Moreover, actual BE values of this variety, at harvest, were almost 20 % higher than the other varieties before defoliation. At the same time, before defoliation, vBA_p was very similar to other varieties. After partial defoliation, *Syrah* presented the lowest vBA_p while both POR and BE remained higher than the remaining varieties. From non-defoliation to partial defoliation, POR and BE increased at the same rate for *Syrah* as with other varieties, while vBA_p increased at a lower rate. This means that, for the variety *Syrah*, although only a low amount of bunches became exposed with the partial defoliation, these bunches represented a higher portion of the total amount of bunches. This leads to the second reason related to the actual yield. The variety *Syrah* presented the lowest yield, more than two times lower than the remaining ones, and consequently, the amount of visible bunch pixels represent very different proportions of total bunches. However, it was still possible to achieve accurate BE estimation results for *Syrah* and *Arinto*, data hints that context information could be a helpful addition to the fruit mass estimation algorithm. In this case, other context information could be considered, such as data regarding plant water status during the growth cycle as it would possibly indicate different levels of canopy density; vigour data, which in many cases is also possible,

today, to be obtained automatically (Gatti *et al.,* 2016; del-Moral-Martínez *et al.,* 2016; Sanz *et al.,* 2018); historical yield data (Riggio *et al.,* 2018; Araya-Alman *et al.,* 2019) as it would lower or increase the expectations of bunch occlusion by leaves in vine images.

The fact that there were no significative differences in the model's statistical measures when applied on the veraison and harvest data sets hints that when attempting to estimate BE, it is possible to collect data, at least, between veraison and harvest, without sacrificing the model's accuracy, which goes in accordance with what was previously observed in Victorino *et al.* (2020). The timing of data collection for yield estimation using image analysis should only be defined by other strategic reasons, such as bunch thinning planning or harvest logistics.

Finally, the validation of model 18 on the combined data set yielded statistical measures that rival the best individual models, especially regarding the bias, which was very close to 0 %. The validated model can be seen as an estimator of the occlusion ratio, as it was previously contemplated by (Nuske *et al.,* 2011a) and can possibly be considered an improvement to that work as it can estimate bunch occlusion by leaves in a fully automatic way. Furthermore, our methodology can be used on all the training systems with vertical plants and does not depend on a specialized imaging system (Riggio *et al.,* 2018). The challenge of bunch occlusion was also very recently studied by Kierdorf *et al.* (2021), who have used a methodology based on generating synthetic images with different cases of bunch occlusion. This approach is a perfect example of how today's machine learning technologies can help face challenges such as the one discussed in our research. However, its application in images collected from non-defoliated vines in field conditions is not yet fully developed. In the present work, instead of machine learning, we focused on image-obtained canopy parameters that are commonly used by growers. In the future, the possibility of combining both strategies can be a very promising approach.

The possible variety dependency observed in Figure 6, where *Syrah* observations are mainly positioned in the lower side of the point cloud, can also be seen in Table 1, where the tBA (vBA in total defoliated vines) of the variety *Syrah* at harvest, for example, presents values that are approximately 20 to 50 % lower than the other varieties. At the same time, actual fruit mass differences are much higher, suggesting that the relationship between tBA and fruit mass varies from case to case. This is possibly caused by two reasons. The first reason is, again, related to differences in bunch morphological traits (OIV, 2009). An example of such a trait is bunch compactness, which has been mentioned in several works as a possible cause of error in bunch weight estimation using image analysis (Aquino *et al.,* 2018b; Hacking *et al.,* 2020). Although this trait changes with different varieties, it can also change with different management practices, flowering and fruit-set conditions and even water availability (Tello and Ibáñez, 2018). The second possible reason is related to the vines lower overall yield and the fact that there is a smaller chance for bunch occlusion by other bunches to occur, a challenge that is not addressed by our model, which by encompassing cases of other varieties, where this bunch occlusion can be higher, creates some misestimations within the *Syrah* variety. Bunch by bunch occlusion can attain significant magnitudes (Nuske *et al.,* 2014b; Victorino *et al.,* 2019) and still requires further research to be automatically obtained, as it remains hard to predict based only on visible image features. A possible factor that might impact bunch by bunch occlusion is how densely positioned bunches are in the canopy, in short, how narrow the fruit zone amplitude is. By knowing the fruit zone amplitude, which can potentially be estimated through image analysis, along with historical yield data, a promising strategy to estimate bunch by bunch occlusion could be computed, which should then be added to the results presented by the approach described in this work.

The multiplying factors to convert tBA into fruit mass (Table 4) are a simplified approach for the area-to-mass conversion. As they are based on the relationship between observed tBA and fruit mass, they encompass several aspects in the same equation, such as bunch occlusion by shoots and by other bunches. As it is also a variety-specific approach, its use should be done with caution when applied to other varieties. Indeed, further research is needed to obtain a robust method to be applied as a general model, possibly by considering other image features and complementary vineyard data. Furthermore, to perform yield estimations with our results, fruit mass estimated at veraison would still be required to be multiplied by a factor that considers berry growth from veraison until harvest. Such an approach, based on historical data, is also used by other methods that attempt to estimate yield at this stage (e.g., Liu *et al.,* 2020; Clingeleffer *et al.,* 2001). Although the main relationship explored in our work (POR + vBA_p vs. BE) was independent of the phenological stage, the area-to-mass conversion is not, as it can be observed by the different slopes between phenological stages (Table 4), most likely caused by the increase in size that generally occurs from veraison until harvest (Coombe and Mccarthy, 2000). Nevertheless, for simplification reasons, and because this challenge goes beyond the scope of the present work, this simplified approach was the option used to obtain the final estimations of fruit mass, which is similar to the approaches presented in, e.g., Lopes *et al.* (2016) and Hacking *et al.* (2019). Even with a simplified area-to-mass conversion, fruit mass estimation results are very promising, with most data sets presenting an absolute error below the strictest estimation error threshold of 5 % mentioned in (Whitty *et al.,* 2017; Table 4). In fact, only the data sets of the varieties *Syrah* (harvest) and *Arinto* (both stages) showed absolute errors above 10 %. Most fruit mass estimation errors are similar to the tBA estimation errors, as expected since the conversion factor was linear. However, the variety *Syrah* (both stages) presented much larger fruit mass estimation errors than tBA errors, which reinforces the idea that there is a need to improve the area-to-mass conversion methodology using extra image features or context data. Regardless, the fruit mass estimation of the combined data set presented an error extremely close to zero, caused by the

compensations between under and overestimations of the different varieties and phenological stages. This error is of similar magnitude and, in some cases outperforms, the ones reported by Liu *et al.* (2020). Furthermore, Liu *et al.* (2020) approach was dependent on individual bunch images taken in field conditions as well as shoot counts, which would require a higher number of steps and images than a vine level imaging strategy like the one proposed in our work.

The approach described in this work seems to be a viable method to estimate bunches hidden by leaves; however, it achieves acceptable accuracy in cases where a considerable portion of bunches are visible. High-density canopies with very low-to-none visible bunches remain a challenge that may only fully be surpassed with advanced sensing such as ultrasounds (Parr *et al.,* 2021) or other devices that can see through leaves, but which are not yet readily available or practical to use in the field conditions.

CONCLUSION

In this study, canopy porosity and visible bunch area in the image were used as proxies for estimating bunch exposure to solve one of the most relevant challenges faced when assessing vineyard yield via image analysis: bunch occlusion by leaves. Our results show that the percentage of occluded bunch area can be estimated using a multiple regression model that includes the variables: canopy porosity and visible bunch area. The obtained pooled model was accurate on data from three varieties at two phenological stages (veraison and full maturation). Final fruit mass estimations presented low errors, similar to state-of-the-art approaches, with the advantage of less effort during image collection. The methodology presented in this work is an important step towards a fully automated non-invasive yield estimation approach, as it improves the estimation of bunches that are occluded by leaves and not visible to scanning devices. Further work is needed to test this methodology in other varieties and sites and to improve area-to-mass conversion models.

ACKNOWLEDGEMENTS

Gonçalo Victorino was supported by the PhD grant SFRH/BD/132305/2017, sponsored by FCT—Fundação para a Ciência e a Tecnologia. We gratefully acknowledge the valuable contributions of master students Guilherme Maia, José Queiroz, Beatrice Carmignani, Giuseppe Samà, Luigi Mauro, Ruben Bonaria and João Mak, who helped with data collection and overall teamwork that made this research possible.

REFERENCES

Abdelghafour, F., Rosu, R., Keresztes, B., Germain, C., & Da Costa, J. P. (2019). A Bayesian framework for joint structure and colour based pixel-wise classification of grapevine proximal images. *Computers and Electronics in Agriculture*, 158(June 2018), 345–357. https://doi.org/10.1016/j.compag.2019.02.017

Aquino, A., Barrio, I., Diago, M. P., Millan, B., & Tardaguila, J. (2018a). vitisBerry: An Android-smartphone application to early evaluate the number of grapevine berries by means of image analysis. *Computers and Electronics in Agriculture*. https://doi.org/10.1016/j.compag.2018.02.021

Aquino, A., Millan, B., Diago, M. P., & Tardaguila, J. (2018b). Automated early yield prediction in vineyards from on-the-go image acquisition. *Computers and Electronics in Agriculture*. https://doi.org/10.1016/j.compag.2017.11.026

Araya-Alman, M., Leroux, C., Acevedo-Opazo, C., Guillaume, S., Valdés-Gómez, H., Verdugo-Vásquez, N., Pañitrur-De la Fuente, C., & Tisseyre, B. (2019). A new localized sampling method to improve grape yield estimation of the current season using yield historical data. *Precision Agriculture*, 20(2), 445–459. https://doi.org/10.1007/s11119-019-09644-y

Austin, C. N., Grove, G. G., Meyers, J. M., & Wilcox, W. F. (2011). Powdery mildew severity as a function of canopy density: Associated impacts on sunlight penetration and spray coverage. *American Journal of Enology and Viticulture*, 62(1), 23–31. https://doi.org/10.5344/ajev.2010.10077

Behroozi-Khazaei, N., & Maleki, M. R. (2017). A robust algorithm based on color features for grape cluster segmentation. *Computers and Electronics in Agriculture*, 142, 41–49. https://doi.org/10.1016/j.compag.2017.08.025

Besselat, B. (1987). Les prévisions de récolte en viticulture. *OENO One*, 21(1), 1–12. https://doi.org/10.20870/oeno-one.1987.21.1.1270

Blom, P. E., & Tarara, J. M. (2009). Trellis tension monitoring improves yield estimation in vineyards. *HortScience*, 44(3), 678–685. https://doi.org/10.21273/HORTSCI.44.3.678

Bramley, R. G. V., Ouzman, J., & Boss, P. K. (2011). Variation in vine vigour, grape yield and vineyard soils and topography as indicators of variation in the chemical composition of grapes, wine and wine sensory attributes. *Australian Journal of Grape and Wine Research*, 17(2), 217–229. https://doi.org/10.1111/j.1755-0238.2011.00136.x

Bramley, R. G. V, & Hamilton, R. P. (2004). Understanding variability in winegrape production systems 2. Within vineyard variation in quality over several vintages. *Australian Journal Of Grape And Wine Research*, 10(1), 32–45. https://doi.org/10.1111/j.1755-0238.2004.tb00006.x

Clingeleffer, P., Dunn, G., Krstic, M. & Martin, S. (2001). Crop development, crop estimation and crop control to secure quality and production of major wine grape varieties: A national approach. *Technical Report*, Grape and Wine Research & Development Corporation, September, Australia..

Coombe, B. G., & Mccarthy, M. G. (2000). Dynamics of grape berry growth and physiology of ripening. *Australian Journal of Grape and Wine Research*, 6(2), 131–135. https://doi.org/10.1111/j.1755-0238.2000.tb00171.x

Cristianini, N., & Shawe-Taylor, J. (2000). An introduction to support vector machines and other kernel-based learning methods. *Cambridge university press*. https://doi.org/10.1017/CBO9780511801389

Cunha, M., Ribeiro, H., & Abreu, I. (2016). Pollen-based predictive modelling of wine production: Application to an arid region. *European Journal of Agronomy*, 73, 42–54. https://doi.org/10.1016/j.eja.2015.10.008

De Bei, R., Fuentes, S., Gilliham, M., Tyerman, S., Edwards, E., Bianchini, N., Smith, J., & Collins, C. (2016). Viticanopy: A free computer app to estimate canopy vigor and porosity for grapevine. *Sensors* (Switzerland). https://doi.org/10.3390/s16040585

del-Moral-Martínez, I., Rosell-Polo, J. R., Company, J., Sanz, R., Escolà, A., Masip, J., Martínez-Casasnovas, J. A., & Arnó, J. (2016). Mapping vineyard leaf area using mobile terrestrial laser scanners: Should rows be scanned on-the-go or discontinuously sampled? *Sensors* (Switzerland), 16(1). https://doi.org/10.3390/s16010119

Diago, M. P., Aquino, A., Millan, B., Palacios, F., & Tardaguila, J. (2019). On-the-go assessment of vineyard canopy porosity, bunch and leaf exposure by image analysis. *Australian Journal of Grape and Wine Research*, 25(3), 363–374. https://doi.org/10.1111/ajgw.12404

Dunn, G. M., & Martin, S. R. (2004). Yield prediction from digital image analysis: A technique with potential for vineyard assessments prior to harvest. *Australian Journal of Grape and Wine Research*. https://doi.org/10.1111/j.1755-0238.2004.tb00022.x

Font, D., Tresanchez, M., Martínez, D., Moreno, J., Clotet, E., & Palacín, J. (2015). Vineyard yield estimation based on the analysis of high resolution images obtained with artificial illumination at night. *Sensors*, 15(4), 8284-8301. https://doi.org/10.3390/s150408284

Fraga, H., & Santos, J. A. (2017). Daily prediction of seasonal grapevine production in the Douro wine region based on favourable meteorological conditions. *Australian Journal of Grape and Wine Research*. https://doi.org/10.1111/ajgw.12278

Gambetta, J. M., Holzapfel, B. P., Stoll, M., & Friedel, M. (2021). Sunburn in Grapes: A Review. *Frontiers in Plant Science*, 11(January). https://doi.org/10.3389/fpls.2020.604691

Gatti, M., Dosso, P., Maurino, M., Merli, M. C., Bernizzoni, F., Pirez, F. J., Platè, B., Bertuzzi, G. C., & Poni, S. (2016). MECS-VINE®: A new proximal sensor for segmented mapping of vigor and yield parameters on vineyard rows. *Sensors* (Switzerland), 16(12). https://doi.org/10.3390/s16122009

Hacking, C., Poona, N., Manzan, N., & Poblete-Echeverría, C. (2019). Investigating 2-D and 3-D proximal remote sensing techniques for vineyard yield estimation. *Sensors (Switzerland), 19*(17). https://doi.org/10.3390/s19173652

Hacking, C., Poona, N., & Poblete-Echeverría, C. (2020). Vineyard yield estimation using 2-D proximal sensing : a multitemporal approach. *Oeno-one* (September), 793–812. https://doi.org/10.20870/oeno-one.2020.54.4.3361

Íñiguez, R., Palacios, F., Barrio, I., & Guti, S. (2021). Impact of Leaf Occlusions on Yield Assessment by Computer Vision in Commercial Vineyards. *Agronomy*, 11(5), 1–13. https://doi.org/10.3390/agronomy11051003

Ivorra, E., Sánchez, A. J., Camarasa, J. G., Diago, M. P., & Tardáguila, J. (2015). Assessment of grape cluster yield components based on 3D descriptors using stereo vision. *Food control*, 50, 273-282. https://doi.org/10.1016/j.foodcont.2014.09.004

Jasse, A., Berry, A., Aleixandre-Tudo, J. L., & Poblete-Echeverría, C. (2021). Intra-block spatial and temporal variability of plant water status and its effect on grape and wine parameters. *Agricultural Water Management*, 246(December 2020), 106696. https://doi.org/10.1016/j.agwat.2020.106696

Jensen, J. R. (1996). *Introductory digital image processing: A remote sensing perspective* (p. 316). Engle- wood Cliffs, NJ, USA: Prentice Hall.

Keller, M., Romero, P., Gohil, H., Smithyman, R. P., Riley, W. R., Casassa, L. F., & Harbertson, J. F. (2016). Deficit irrigation alters grapevine growth, physiology, and fruit microclimate. *American Journal of Enology and Viticulture*, 67(4), 426–435. https://doi.org/10.5344/ajev.2016.16032

Kierdorf, J., Weber, I., Kicherer, A., Zabawa, L., Drees, L., & Roscher, R. (2021). Behind the leaves -- Estimation of occluded grapevine berries with conditional generative adversarial networks. May 2021. http://arxiv.org/abs/2105.10325

Krasnow, M. N., Matthews, M. A., Smith, R. J., Benz, J., Weber, E., & Shackel, K. A. (2010). Distinctive symptoms differentiate four common types of berry shrivel disorder in grape. *California Agriculture*, 64(3), 155–159. https://doi.org/10.3733/ca.v064n03p155

Lecun, Y., Bengio, Y., & Hinton, G. (2015). Deep learning. *Nature*. https://doi.org/10.1038/nature14539

Liu, S., Cossell, S., Tang, J., Dunn, G., & Whitty, M. (2017). A computer vision system for early stage grape yield estimation based on shoot detection. *Computers and Electronics in Agriculture*, 137, 88–101. https://doi.org/10.1016/j.compag.2017.03.013

Liu, S., Marden, S., & Whitty, M. (2013). Towards automated yield estimation in viticulture. In *Proceedings of the Australasian Conference on Robotics and Automation*, Sydney, Australia (Vol. 24, pp. 2-6).

Liu, S., Zeng, X., & Whitty, M. (2020). A vision-based robust grape berry counting algorithm for fast calibration-free bunch weight estimation in the field. *Computers and Electronics in Agriculture*, 173(December 2019), 105360. https://doi.org/10.1016/j.compag.2020.105360

Lorenz, D. H., Eichhorn, K. W., Bleiholder, H., Klose, R., Meier, U., & Weber, E. (1995). Growth Stages of the Grapevine: Phenological growth stages of the grapevine (Vitis vinifera L. ssp. vinifera)—Codes and descriptions according to the extended BBCH scale. *Australian Journal of Grape and Wine Research*, 1(2), 100-103. https://doi.org/10.1111/j.1755-0238.1995.tb00085.x

Lopes, C. M., Egipto, R., Zarrouk, O., & Chaves, M. M. (2020). Carry-over effects on bud fertility makes early defoliation a risky crop-regulating practice in Mediterranean vineyards. *Australian Journal of Grape and Wine Research*, 26(3), 290–299. https://doi.org/10.1111/ajgw.12437

Lopes, C. M., Graça, J., Sastre, J., Reyes, M., Guzmán, R., Braga, R., ... & Pinto, P. A. (2016). Vineyard yeld estimation by VINBOT robot-preliminary results with the white variety Viosinho. In *Proceedings 11th Int. Terroir Congress*. Jones, G. and Doran, N.(eds.), pp. 458-463. Southern Oregon University, Ashland, USA. Jones, G.; Doran, N.(eds.).

Lopes, C., Torres, A., Guzman, R., Graca, J., Reyes, M., Victorino, G., Braga, R., Monteiro, A., & Barriguinha, A. (2017). Using an unmanned ground vehicle to scout vineyards for non-intrusive estimation of canopy features and grape yield. In *Proceedings 20th GiESCO International Meeting*, 2, 16–21.

Martínez-Lüscher, J., Chen, C. C. L., Brillante, L., & Kurtural, S. K. (2020). Mitigating Heat Wave and Exposure Damage to "Cabernet Sauvignon" Wine Grape With Partial Shading Under Two Irrigation Amounts. *Frontiers in Plant Science*, 11(November), 1–15. https://doi.org/10.3389/fpls.2020.579192

Milella, A., Marani, R., Petitti, A., & Reina, G. (2019). In-field high throughput grapevine phenotyping with a consumer-grade depth camera. *Computers and Electronics in Agriculture*, 156(May 2018), 293–306. https://doi.org/10.1016/j.compag.2018.11.026

Nuske, S., Achar, S., Gupta, K., Narasimhan, S., & Singh, S. (2011a). Visual yield estimation in vineyards: experiments with different varietals and calibration procedures. *Robotics Institute, Carnegie Mellon University Technical Report*: CMURI-TR-11-39, Dec.

Nuske, S., Achar, S., Bates, T., Narasimhan, S., & Singh, S. (2011b). Yield estimation in vineyards by visual grape detection. In *Proceedings 2011 IEEE/RSJ International Conference on Intelligent Robots and Systems* (pp. 2352-2358). IEEE. https://doi.org/10.1109/IROS.2011.6095069

Nuske, S., Gupta, K., Narasimhan, S., & Singh, S. (2014a). Modeling and calibrating visual yield estimates in vineyards. *Springer Tracts in Advanced Robotics*, 92, 343–356. https://doi.org/10.1007/978-3-642-40686-7_23

Nuske, S., Wilshusen, K., Achar, S., Yoder, L., & Singh, S. (2014b). Automated visual yield estimation in vineyards. *Journal of Field Robotics*. https://doi.org/10.1002/rob.21541

OIV (2009). Organisation Internationale de la Vigne et du Vin. Description of world vine varieties. 560.

Parr, B., Legg, M., Bradley, S., & Alam, F. (2021). Occluded grape cluster detection and vine canopy visualisation using an ultrasonic phased array. *Sensors*, 21(6), 1–20. https://doi.org/10.3390/s21062182

Pérez-Zavala, R., Torres-Torriti, M., Cheein, F. A., & Troni, G. (2018). A pattern recognition strategy for visual grape bunch detection in vineyards. *Computers and Electronics in Agriculture*, 151, 136–149. https://doi.org/10.1016/j.compag.2018.05.019

Pfeiffer, S. A., Guevara, J., Cheein, F. A., & Sanz, R. (2018). Mechatronic terrestrial LiDAR for canopy porosity and crown surface estimation. *Computers and Electronics in Agriculture*. https://doi.org/10.1016/j.compag.2018.01.022

Riggio, G., Fantuzzi, C., & Secchi, C. (2018). A Low-Cost Navigation Strategy for Yield Estimation in Vineyards. In *Proceedings 2018 IEEE International Conference on Robotics and Automation (ICRA),* 2200–2205. https://doi.org/10.1109/ICRA.2018.8462839

Rudolph, R., Herzog, K., Töpfer, R., & Steinhage, V. (2018). Efficient identification, localization and quantification of grapevine inflorescences in unprepared field images using fully convolutional networks. arXiv preprint arXiv:1807.03770.

Sanz, R., Llorens, J., Escolà, A., Arnó, J., Planas, S., Román, C., & Rosell-Polo, J. R. (2018). LIDAR and non-LIDAR-based canopy parameters to estimate the leaf area in fruit trees and vineyard. *Agricultural and Forest Meteorology*. https://doi.org/10.1016/j.agrformet.2018.06.017

Seng, K. P., Ang, L. M., Schmidtke, L. M., & Rogiers, S. Y. (2018). Computer vision and machine learning for viticulture technology. *IEEE Access*, 6, 67494–67510. https://doi.org/10.1109/ACCESS.2018.2875862

Smart, R. E. (1987). Influence of light on composition and quality of grapes. *Acta Horticulturae*, 206, 37–48. https://doi.org/10.17660/ActaHortic.1987.206.2

Smart, R. E. (1988). Shoot spacing and canopy light microclimate. *American Journal of Enology and Viticulture*, 39(4), 325–333.

Smart, R. and Robinson, M. (1991) *Sunlight into the wine. A handbook for winegrape canopy management*. (Winetitles: Adelaide).

Taylor, J. A., Dresser, J. L., Hickey, C. C., Nuske, S. T., & Bates, T. R. (2018). Considerations on spatial crop load mapping. *Australian Journal of Grape and Wine Research*. https://doi.org/10.1111/ajgw.12378

Teixeira, G., Monteiro, A., Santos, C., & Lopes, C. M. (2018). Leaf morphoanatomy traits in white grapevine cultivars with distinct geographical origin. *Ciencia e Tecnica Vitivinicola*, 33(1), 90–101. https://doi.org/10.1051/ctv/20183301090

Tello, J., & Ibáñez, J. (2018). What do we know about grapevine bunch compactness? A state-of-the-art review. In *Australian Journal of Grape and Wine Research* (Vol. 24, Issue 1, pp. 6–23). Blackwell Publishing Ltd. https://doi.org/10.1111/ajgw.12310

Victorino, G., Braga, R., & Lopes, C. M. (2017). The effect of topography on the spatial variability of grapevine vegetative and reproductive components. *Actas Portuguesas de Horticultura*, 29, 510–516.

Victorino, G., Braga, R., Santos-Victor, J., & Lopes, C. M. (2020). Yield components detection and image-based indicators for non-invasive grapevine yield prediction at different phenological phases. *OENO One*. 54(4).833-848. https://doi.org/10.20870/oeno-one.2020.54.4.3616;

Victorino, G., Maia, G., Queiroz, J., Braga, R., Marques, J., Santos-Victor, J., & Lopes, C. (2019). Grapevine yield prediction using image analysis - improving the estimation of non-visible bunches. In *Proceedings EFITA 2019: Digitizing Agriculture*.

Whitty, M., Liu, S., Cossell, S., Jayakody, H., Woods, M., Tang, J., Singh, S., Van Kerk Oerle, P., Wiseham, D., Liu, S., Davidson, A., Stocco, T., Jarrett, J., Jarrett, P., Wotton, C., Shepherd, J., Lim, S., Petrie, P., & Dunn, G. (2017). Improved yield estimation for the Australian wine industry. In *Wine Australia*. Department of Primary Industries NSW & University of NSW, November, 167.